Chemical Physics Letters 749 (2020) 137434

Contents lists available at ScienceDirect

Chemical Physics Letters

journal homepage: www.elsevier.com/locate/cplett

Research paper

Highly stable viologens-based electrochromic devices with low operational voltages utilizing polymeric ionic liquids

Xiuxiu Wang[a,b], Lijuan Guo[b], Shaokui Cao[a,*], Weizhen Zhao[b,*]

[a] School of Materials Science and Engineering, Zhengzhou University, Henan 450001, PR China
[b] Beijing Key Laboratory of Ionic Liquids Clean Process, CAS Key Laboratory of Green Process and Engineering, Institute of Process Engineering, Chinese Academy of Sciences, Beijing 100190, PR China

HIGHLIGHTS

- Asymmetrical 1-alkyl-1′-aryl substituted viologen and polyviologen were synthesized.
- Viologens-based electrochromic devices with polymeric ionic liquids were assembled.
- The ECDs exhibited well electrochromic behavior.
- Cyclic stability over 96% of initial transmittance change after 4000 cycles of switching.

ARTICLE INFO

Keywords:
Electrochromism
Electrochemical displays
Ion gel electrolytes
Viologens
Polymeric ionic liquids

ABSTRACT

In this work, we proposed an effective route of introducing poly(ionic liquid) (PIL) gel as electrolyte to suppress dimer formation of viologen radical cation during switching in electrochromic devices (ECDs). The ECDs were fabricated based on ion gels consisting of various viologens, PIL and ferrocene (Fc). We found that incorporation of PIL contributed to the suppression of dimer production. The suppression of dimer formation can provide ECDs with improved colouration efficiencies, faster switching times, longer cycle lives, and potentially reduced costs. The results showed that an excellent cyclic stability over 96% of initial transmittance change after 4000 cycles of switching.

1. Introduction

Electrochromic (EC) materials have the ability to reversibly alter their optical characteristics via redox reactions driven by an application voltage bias [1-3]. Therefore, EC materials have been widely used in electrochemical applications such as anti-glare rear view mirrors, sensors, military equipment camouflage, information displays, electrochemical device and so on [4,5]. For all applications, the device performance highly depends on the electrochemical and optical properties of EC materials.

EC materials such as metal oxides [6,7], conducting polymers [8,9], organic small molecules with redox activity [10–12], and metal complexes [13] have been reported. Among them, viologens, N,N-substituted bipyridiniums, have received wide attention since their remarkable and reversible color contrast from colorless to blue or violet during their first redox process [14]. Viologens possess three redox states, including neutral state (V^0), deep colored radical cation state ($V^{+\cdot}$) and colorless dication state (V^{2+}) [15,16]. The optical characteristics of viologens could be easily tuned with different substituent groups on bipyridinums [17]. However, the long-term stability of viologen-based solution-type ECDs suffers from the poor solubility of $V^{+\cdot}$ [18]. The $V^{+\cdot}$ tends to form dimer via spin-pairing during the operation and results in an irreversible bleaching process [19]. To avoid the dimerization of viologen, asymmetric molecular modification of viologen and gel-based ECDs have been considered as two feasible method [20–22]. On the other hand, in general, ECDs containing viologens in a liquid electrolyte suffer from not only the side reactions mentioned above but also the possibility of electrolyte leakage [23]. Polymer gel electrolytes (PGEs), which are widely used in supercapacitors [24], actuators [25] and dye-sensitized solar cells (DSSCs) [26], are of great potential for ECDs. However, one important challenge for display applications of ECDs based on electrolyte gels is their low ionic conductivity (10^{-3}–10^{-1} mS/cm) [27]. Therefore, many research groups has focused on how to improve the conductivity [28,29]. Timothy P. Lodge reported an ion gel, a composite of ABA triblock copolymer with an IL-soluble B block and IL-insoluble A blocks and room

* Corresponding authors.
E-mail addresses: caoshaokui@zzu.edu.cn (S. Cao), wzzhao@ipe.ac.cn (W. Zhao).

https://doi.org/10.1016/j.cplett.2020.137434
Received 18 March 2020; Received in revised form 30 March 2020; Accepted 31 March 2020
Available online 01 April 2020
0009-2614/

temperature ionic liquids (ILs), possessed higher ionic conductivity (1–10 mS/cm) than that of conventional PGEs (10^{-3}–10^{-1} mS/cm) [30]. Additionally, ion gels consisting of room temperature ILs and random copolymers [31,32] or star copolymers [33] have been developed. Here, the ion gels exhibited high capacitance, exceptional thermal and chemical stability, insignificant vapor pressure and wide electrochemical window [34–36]. Therefore, this is an effective strategy for ECDs with high performance by introducing ionic liquid into copolymers to obtain an ion gel. Ion gels could be considered as promising candidates in a range of electrochemical electronics.

In this study, the strategy was extended that we introduced poly (ionic liquid) as ion gel into ECDs to prevent leakage while enhancing the cyclic stability by avoiding the formation of viologen dimer. Poly(1-vinyl-3-butylimidazolium bromide) (poly(VBImBr)) was synthesized and employed as electrolyte gel. We prepared diheptyl viologen bis-(hexafluorophosphate) ($DHV(PF_6)_2$), heptyl vinyl benzyl viologen bis (hexafluorophosphate) ($HBV(PF_6)_2$) and poly(heptyl vinyl benzyl viologen bis(hexafluorophosphate)) ($poly(HBV(PF_6)_2)$) as electrochromic chromophores for systematical investigation. All homogeneous EC ion gels were prepared by blending poly(VBImBr), ferrocene (Fc) and various viologens. Then, the device were assembled by sandwiching the obtained ion gel between two ITO conducting glasses. The influence of viologen substituents on ECDs properties was studied and compared in terms of kinetic stability, spectroelectrochemistry, and cyclic voltammetry as well.

2. Experimental section

2.1. Materials

Ethanol absolute (≥99.8%), potassium bromide (KBr, ≥ 99.5%) and 2,2′-azobis(isobutyronitrile) (AIBN, 99%) were purchased from Aladdin. Vinyl benzyl chloride (VBC, 90%) was purchased from Sigma-Aldrich. 4,4′-bipyridine (98%), heptyl bromide (98%), N,N-dimethylformamide (DMF, 99.5%), ferrocene (Fc, 95%) potassium hexafluorophosphat (KPF_6, 95%) and propylene carbonate (PC, 98%) were provided by TCI. 1-vinyl-3-butylimidazolium bromide (VBImBr, 99%) was obtained from Lanzhou Oricko Chemical Co., Ltd. Acetonitrile (ACN, AR), acetone (AR) and diethyl ether (AR) were purchased from Beijing Chemical Works. Deionized water (DIW) was used throughout this study. The ITO substrate (sheet resistance is < 7 Ω/□) was obtained from South China Science and Technology Co., Ltd, Shenzhen. All the materials were used as received without any further purification except the ITO conducting glass which was washed with deionized water, acetone and ethanol for 10 min under sonication, respectively.

2.2. Synthesis of poly(1-vinyl-3-butylimidazolium bromide) (poly (VBImBr))

Poly(VBImBr) was prepared following previous investigation (Scheme 1) [37]. Firstly, the poly(VBImBr) homopolymer was synthesized through radical polymerization of VBImBr in ethanol with AIBN as an initiator. AIBN (5 wt‰ with respect to monomer) was injected to the ethanol solution of VBImBr slowly, and the reaction mixture was stired vigorously at 70 °C for 9 h under nitrogen. Subsequently, the raw product was separated by precipitating into acetone, filtering the resulting precipitate and washing it with acetone for several times. the obtained yellowish poly(VBImBr) solid was dried in a vacuum oven at 40 °C for 24 h. IR (cm^{-1}, KBr): 3442 (s), 3068 (m), 2961 (s), 2869 (s), 1660 (s), 1546 (m), 1456 (m), 1163 (m), 746 (m). ^{1}H NMR (600 MHz, DMSO, ppm): δ 8.45 – 7.45 (m, 4H), 4.15 (d, J = 24.2 Hz, 2H), 1.59 (d, J = 302.2 Hz, 5H), 0.95 (s, 3H).

2.3. Synthesis of the symmetric, asymmetric viologen and polyviologen

The synthetic route of symmetric diheptyl viologen (DHV), alkyl-aryl asymmetric viologen (HBV) and polyviologen (PHBV) were depicted in Scheme 1. The synthetic procedure included two-step section wherein the aryl or alkyl substituent was first bonded through S_N2 substitution reaction, whereas the relative hydrophobicity viologens were second obtained through an anion exchange. Symmetric diheptyl viologen bis-(hexafluorophosphate) ($DHV(PF_6)_2$) was synthesized following the literature [38].

2.3.1. Synthesis of heptyl vinyl benzyl viologen bis(hexafluorophosphate) ($HBV(PF_6)_2$)

As reported in the literature [39], monoheptyl viologen bromide (MHVBr) was synthesized as follows: a mixture of 4,4′-bipyridine (1.825 g, 12 mmol) and heptyl bromide (2 g, 10 mmol) was dissolved in ACN (20 ml) and stirred at 50 °C for 72 h. MHVBr was isolated from the mixed solution by filtering, washed with diethyl ether and dried under vacuum at 50 °C for 24 h. Then, the arylation of MHVBr utilizing DMF as a solvent to prepare heptyl vinyl benzyl viologen bromide chloride (HBVBrCl) was conducted in the similar fashion as MHVBr. $HBV(PF_6)_2$ was synthesized by an anion exchange with the HBVBrCl and excess KPF_6 dissolved in DIW. The white precipitated $HBV(PF_6)_2$ was obtained, separated through filtration, and washed with DIW after stirring for 24 h. Ultimately, $HBV(PF_6)_2$ was collected after drying under vacuum at 50 °C for 24 h. IR (cm^{-1}, KBr): 3087 (m), 2924 (s), 2854 (s), 1635 (s), 1509 (m), 1454 (s), 920 (m), 828 (s), 726 (m). ^{1}H NMR (600 MHz, DMSO, ppm): δ 9.49 (d, J = 6.9 Hz, 4H), 9.37 (t, J = 7.9 Hz, 4H), 8.78 – 8.71 (m, 2H), 7.62 – 7.54 (m, 2H), 6.75 (dd, J = 17.6, 11.0 Hz, 1H), 5.90 (d, J = 16.3 Hz, 2H), 5.33 (d, J = 11.0 Hz, 2H), 4.67 (t, J = 7.4 Hz, 2H), 1.97 (s, 2H), 1.38 – 1.16 (m, 8H), 0.86 (t, J = 7.0 Hz, 3H).

2.3.2. Synthesis of poly(heptyl vinyl benzyl viologen bis (hexafluorophosphate)) ($poly(HBV(PF_6)_2)$)

$Poly(HBV(PF_6)_2)$ was synthesized following the literature [40]. In detail, the radical polymerization reaction of HBVBrCl occurred in DMF at 70 °C for 10 h with AIBN as an initiator. Poly(HBVBrCl) was isolated from the mixed solution by filtering, washed with diethyl ether and then dried under vacuum at 50 °C for 24 h. $Poly(HBV(PF_6)_2)$ was synthesized using the same process with $HBV(PF_6)_2$. IR (cm^{-1}, KBr): 3086 (m), 2924 (s), 2854 (s), 1635 (s), 1557 (m), 1504 (m), 1448 (m), 809 (m), 728 (m). ^{1}H NMR (600 MHz, DMSO, ppm): δ 9.42 (d, J = 71.2 Hz, 4H), 8.74 (s, 4H), 7.58 (s, 4H), 6.75 (dd, J = 17.4, 10.8 Hz, 1H), 5.90 (d, J = 17.7 Hz, 2H), 5.33 (dd, J = 11.7, 7.0 Hz, 2H), 4.67 (s, 2H), 2.07 – 1.79 (m, 2H), 1.47 – 1.06 (m, 8H), 0.91 – 0.71 (m, 3H).

2.4. Device fabrication

All homogeneous EC gels consisting of poly(VBImBr) and PC at a weight fraction of 1:4 were completely dissolved at 40 °C. Subsequently, Fc and viologen compounds at a weight fraction of 3:20 were introduced into the above solution. The resulting EC gels were then deposited on the ITO conducting glass by blade coating. Another ITO conducting glass was placed in reverse on the gel quickly and two ITO conducting glasses were laminated using a cell gap of 60 μm double-sided tape firmly, as was demonstrated in Scheme 2.

2.5. Characterization

The chemical structures of poly(VBImBr) and viologen compounds synthesized in this work were confirmed with ^{1}H NMR (Avance III 600) and FTIR (Nicolet 380, Thermo Electron) instrument. The IR and ^{1}H NMR spectrum of them were shown in Figs. S1–S4. The applied square wave voltage was supplied by a potentiostat (MS-605D, Maisheng). The cyclic voltammogram (CV) curves of DHV, HBV and PHBV-containing ECDs were recorded on an electrochemical workstation (CHI 660E, Shanghai Chenhua CH Instruments, Inc.) under two-electrode system configuration. The UV–vis absorption spectrum of the devices were

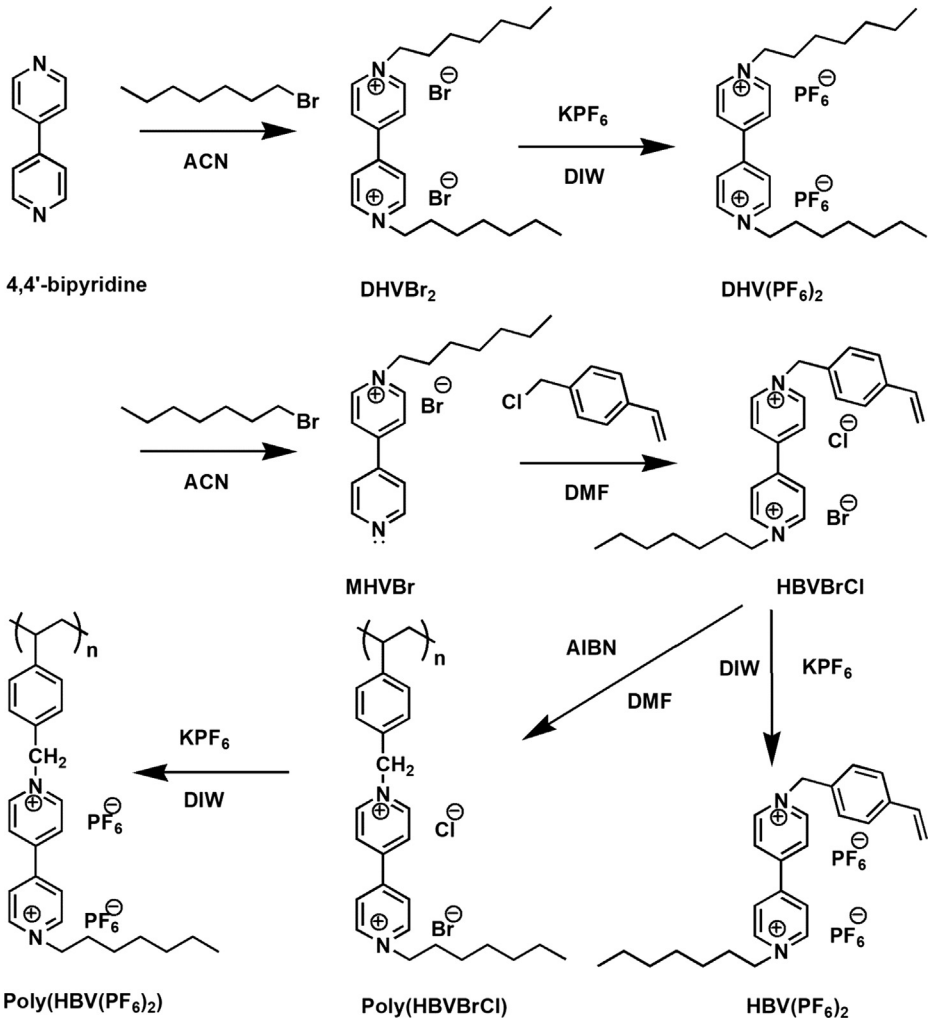

Scheme 1. Synthetic route for symmetric diheptyl viologen (DHV), asymmetric viologen (HBV) and polyviologen (PHBV).

recorded in transmission mode by using an UV–vis sprctrometer (UV-2550) within wavelengths of the visible range at different applied voltages. Dynamic transmittance change curves of the devices in specific wavelength were measured by using a combination of the potentiostat and UV–vis sprctrometer (UV-2550) under two-electrode system configuration.

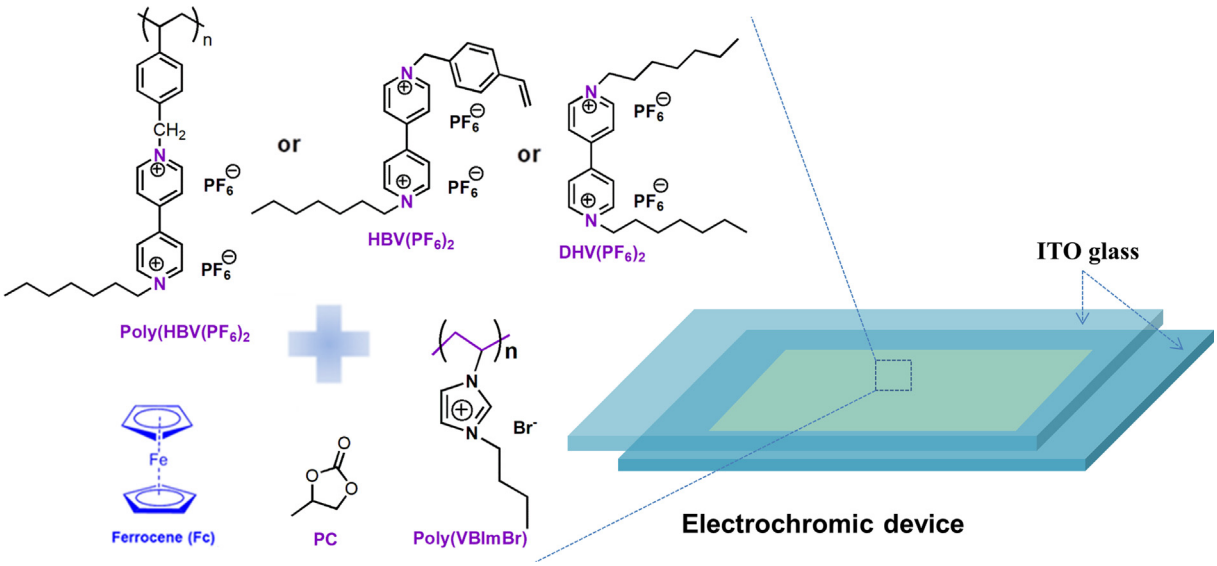

Scheme 2. The viologen-based ECDs architecture.

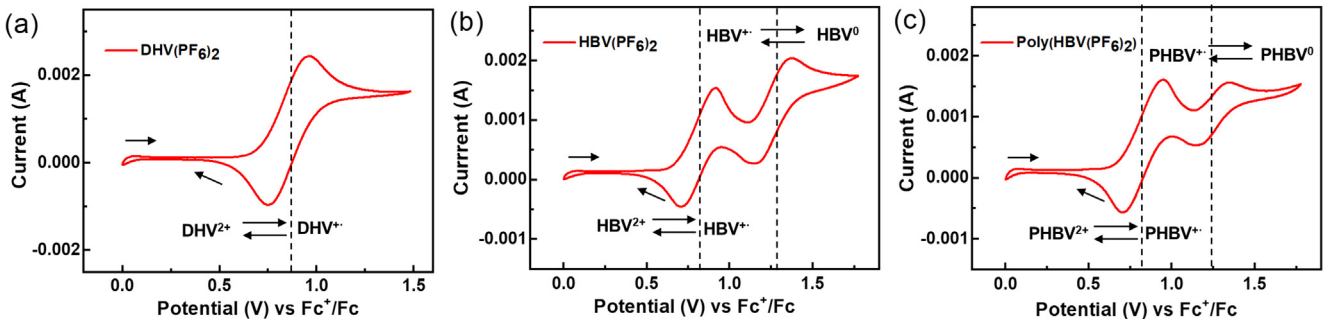

Fig. 1. Cyclic voltammograms of (a) DHV, (b) HBV, and (c) PHBV-containing ECDs under two-electrode system configuration at a rate of 20 mV/s. Fc served as both anodic species and internal standard.

Table 1
Summarized electrochemical properties of DHV, HBV and PHBV-containing ECDs.

Viologen	Peak potential, V vs Fc^+/Fc		Peak current, mA	
	E_{pa}^1/E_{pc}^1	E_{pa}^2/E_{pc}^2	I_{pa}^1/I_{pc}^1	I_{pa}^2/I_{pc}^2
$DHV(PF_6)_2$	0.96/0.75	–	2.23/-2.19	–
$HBV(PF_6)_2$	0.91/0.71	1.36/1.15	1.27/-0.78	0.75/0.82
$Poly(HBV(PF_6)_2)$	0.95/0.71	1.34/1.15	1.37/-1.00	0.36/0.55

3. Results and discussion

3.1. Electrochemical characteristics of viologen-based ECDs

To understand the electrochemical characteristics of ion gel-based ECDs with DHV, HBV and PHBV, the cyclic voltammograms (CV) curves were conducted at scanning rate of 20 mV/s (Fig. 1). Fc was introduced in viologen-based ECDs as both anodic species and internal standard material, the redox potentials of these viologens were obtained on the basis of that of the Fc^+/Fc, which corresponded to the

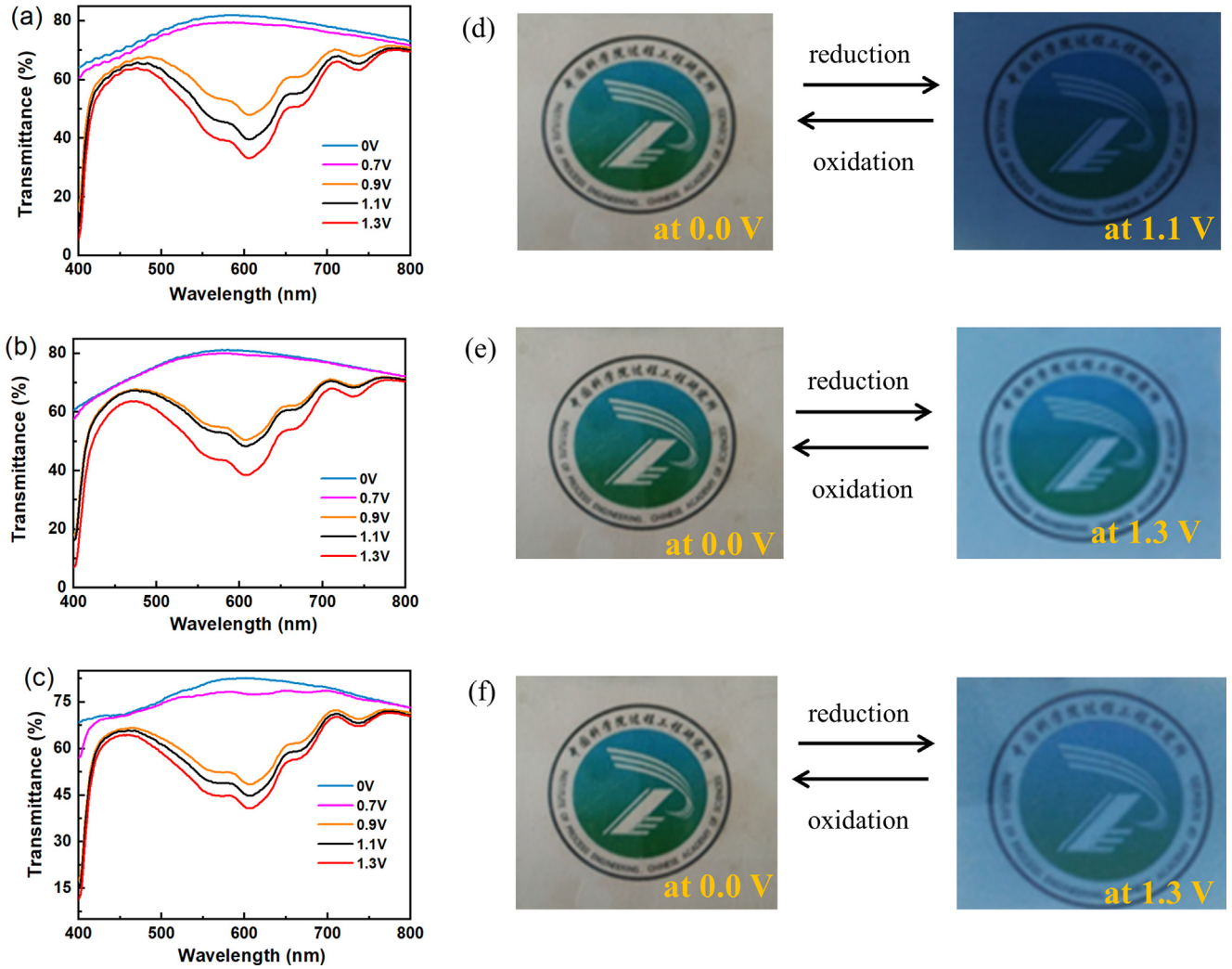

Fig. 2. The UV–vis absorption spectrum in transmission mode at various applied potentials and the photographs of the colored and bleached (a) DHV, (b) HBV, and (c) PHBV-containing ECDs states.

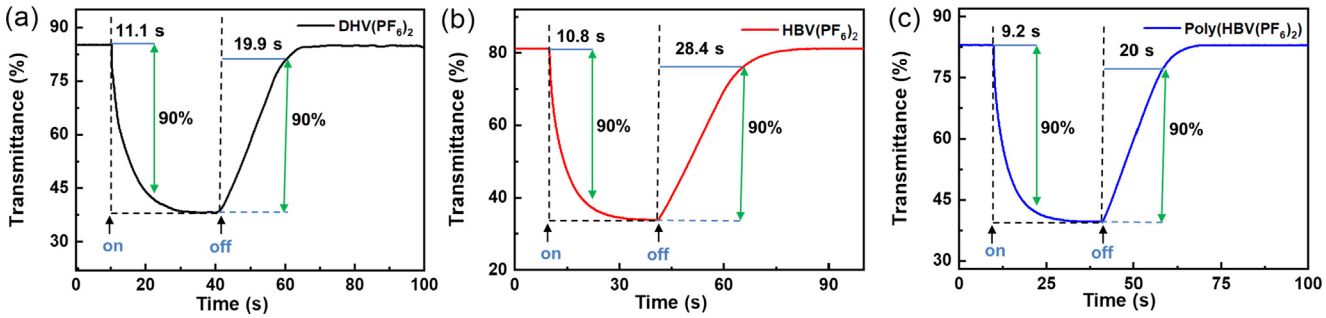

Fig. 3. Transient transmittance profiles of (a) DHV/Fc ECD at 606 nm and 1.1 V, (b) HBV/Fc ECD at 608 nm and 1.3 V, and (c) PHBV/Fc ECD at 606 nm and 1.3 V, respectively.

Table 2
Electrochemical properties of DHV, HBV and PHBV-containing ECDs.

Viologen	λ_{max} (nm)	η [a] (cm^2 /C)	△T (%)	Switching time (s)	
				Colored [b]	Bleached [c]
$DHV(PF_6)_2$	606	109.8	47.7	11.1	19.9
$HBV(PF_6)_2$	608	106.2	45.4	10.8	28.4
$Poly(HBV(PF_6)_2)$	606	105.7	41.1	9.2	20

The applied square wave voltage between 0 and 1.1 V for DHV-containing ECDs, and between 0 and 1.3 V for HBV, and PHBV-containing ECDs.

[a] Coloration efficiency (η) was determined by utilizing the measured charge density.

[b] The requisite time to achieve 90% ($\triangle T_{90\%}$) of the total transmittance change for coloration.

[c] The requisite time to achieve 90% ($\triangle T_{90\%}$) of the total transmittance change for bleaching.

requisite voltage for the coloration of the devices. The redox reaction of $DHV^{2+}/DHV^{+\cdot}$ (Fig. 1a), $HBV^{2+}/HBV^{+\cdot}$ (Fig. 1b) and $PHBV^{2+}/PHBV^{+\cdot}$ (Fig. 1c) couples occurred at 0.86 V, 0.81 V and 0.83 V (vs. Fc^+/Fc), respectively. Here, the reduction of DHV^{2+} only to generate the reduced state ($DHV^{+\cdot}$) along with one electron transferring. In Fig. 1b and c, the first cathodic peak of the HBV and PHBV-containing EC gels registered at 0.71 V (vs. Fc^+/Fc) was correlated with the radical cation ($V^{+\cdot}$), generated as a result of the reduction of the divalent cation (V^{2+}), while the second cathodic peak of them observed at 1.15 V (vs. Fc^+/Fc) was related to the neutral state (V^0) obtained through the second reduction of the divalent cation. The electrochemical characteristics obtained through the CV measurements were given in Table 1. The redox peak of $DHV^{2+}/DHV^{+\cdot}$ was shown with high reversibility (i_{pa}/i_{pc}~1.02). In contrast, asymmetric HBV and PHBV exhibited low reversibility of redox behaviors (Fig. 1b and c). The i_{pa}/i_{pc} was only ~1.63 ($HBV^{2+}/HBV^{+\cdot}$) and ~1.37 ($PHBV^{2+}/PHBV^{+\cdot}$) respectively. The high reversibility meant excellent cyclic stability. This results indicated that symmetric DHV was more stable in ECDs with poly(ionic liquid) as electrolyte. This was also consistent with the results of cycle stability characterization (Fig. 4). However, the electrochemical behavior of symmetric and asymmetric heptyl viologen in ECDs with poly(ionic liquid) gel electrolyte was different from that reported one in solution-type ECDs [41]. The reason may be that the introduced PIL can effectively suppress the dimerization of viologen radical cation.

3.2. Spectroelectrochemistry properties of viologen-based ECDs

Since the optical characteristics of viologen-based ECDs relied on the applied voltage, the UV–vis absorption spectrum of the devices were measured in transmission mode within wavelengths of the visible range at different applied voltages. There was no obvious change in the in UV–vis spectra of DHV-including ECDs (Fig. 2a) up to 0.7 V, whereas a characteristic peak at 606 nm originated from the generated $DHV^{+\cdot}$ was observed at 0.9 V, which was in good agreement with coloration voltage estimated by cyclic voltammograms shown in Fig. 1a. Because the larger applied voltages accelerated the generation of $DHV^{+\cdot}$, giving rise to a higher $DHV^{+\cdot}$ concentration, more obvious and intense peak was detected, but the characteristic peak was unchanged at 606 nm, illustrating the major colored species was $DHV^{+\cdot}$ in DHV-including ECDs. Additionally, the ECD showing blue colored state at 1.1 V coincided with the presence of $DHV^{+\cdot}$ (Fig. 2d). Similar to the UV–vis spectra of DHV-including ECDs, the transmittance peak of HBV and PHBV-containing ECDs gradually increased with increasing applied voltage as depicted in Fig. 2b and c, respectively, and stronger transmmittance peaks were found at 608 and 606 nm. The photographs of HBV and PHBV-containing ECDs in the colored and bleached states were demonstrated in the image of Fig. 2e and f, respectively.

3.3. Optical contrast and response time of viologen-based ECDs

The slow coloration rate was a major limitation to the commercialization of ECDs as display materials, even though ECDs possessed many advantages [42]. Therefore, the redox kinetics was a significant factor to the development of ECDs. To study the coloration and bleaching kinetics for DHV, HBV and PHBV-containing ECDs, the transient

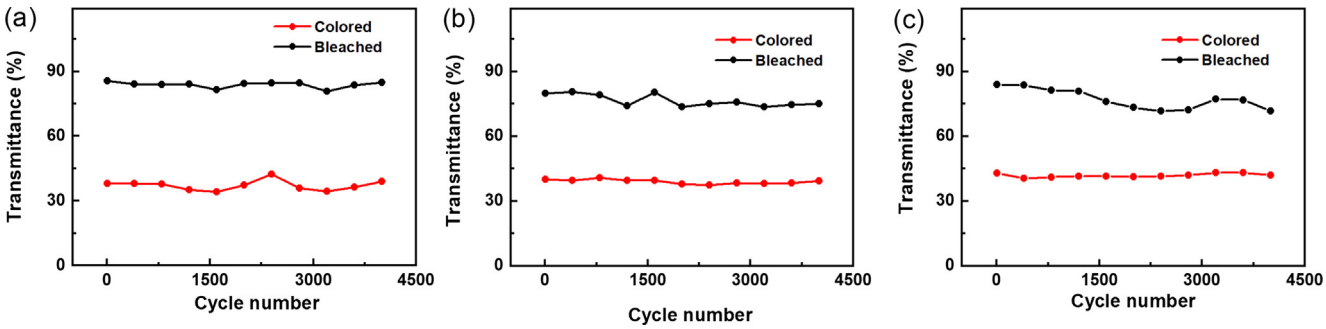

Fig. 4. Cycling stabilities of (a) DHV/Fc ECD at 606 nm and 1.1 V, (b) HBV/Fc ECD at 608 nm and 1.3 V, and (c) PHBV/Fc ECD at 606 nm and 1.3 V, respectively.

Table 3
Summarized the electrochemical properties of viologen-based ECDs utilizing liquid, gel or solid electrolyte.

ECD system	BzV/Fc	HV/TMPD	VRS/TMPD	HV/TMPD	HERFV/Fc	DHV/Fc
Type	liquid	liquid	liquid	solid	gel	gel
λ_{max} (nm)	605	615	620	620	604	606
V_b/V_c (V)	0/1.2	0/1.0	0/0.4	0/0.9	0/-1.0	0/1.1
t_b/t_c[a] (s)	2.2/2.1	2.5/8.0	2.7/2.7	5.2/2.1	15/22	11.1/19.9
△T (%)	53.8	75.5	62.6	60.1	35.4	46.8
Cyclic stability[b] (%)	44.6 after 5000 cycles	100 after 100 cycles	72.4 after 1000 cycles	79.6 after 2000 cycles	91.5 after 2000 cycles	96.0 after 4000 cycles
Ref	[43]	[44]	[45]	[46]	[47]	This work

[a] The requisite time to achieve 90% ($\triangle T_{90\%}$) of the total transmittance change for coloration/ bleaching.
[b] Retained percentage of its initial ΔT.

transmittance curves were measured at either 606 nm or 608 nm, respectively. The requisite time to achieve 90% ($\triangle T_{90\%}$) of the total transmittance change was 11.1 s for coloration of the DHV/Fc ECD, as shown in Fig. 3a. When coloration voltage (1.1 V for 30 s) was applied to two ITO-coated substrates, DHV^{2+} and Fc were consumed on the cathode and anode, respectively, which resulted in the generation of the reduced state ($DHV^{+\cdot}$) and Fc^+. The diffusion of the radical cation ($DHV^{+\cdot}$) and Fc^+ from the surfuce of two ITO-coated electrodes to the center of the EC gel was performed owing to the concentration gradient. Ultimately, these two species encountered and spontaneous electron-transfer reaction occurred because of the negative △G for this reaction, which was in agreement with the bleaching process of the devices under open-circurt condition. Therefore, the requisite time to achieve 90% ($\Delta T_{90\%}$) of the total transmittance change was 19.9 s for bleaching of the DHV/Fc ECD under open-circurt condition. The HBV/Fc ECD and PHBV/Fc ECD showed similar EC behavior (Fig. 3b and c): the times for $\Delta T_{90\%}$ for coloration at 1.3 V were 10.8 s and 9.2 s, respectively, and the times for $\Delta T_{90\%}$ for bleaching under open-circurt condition were 28.4 s and 20 s, respectively. According to the definition of optical contrast, optical contrast of three kinds of ECDs was 47.7% (DHV/Fc ECD), 45.4% (HBV/Fc ECD), 41.1% (PHBV/Fc ECD), respectively, while the coloration efficiency (η) for them was estimated to be 109.8 cm^2 /C, 106.2 cm^2 /C, 105.7 cm^2 /C respectively. The current-time curves of $DHV(PF_6)_2$, $HBV(PF_6)_2$ and $poly(HBV(PF_6)_2)$ were shown in Fig. S5. The performance of ECDs was summarized in Table 2. It was worth to mention that the sharp curves indicated fast switching in respoonse to the applied potential bias. Additionally, excellent reversibility of coloration/bleaching cycles was also seen in Fig. 3. Specifically, the bleached transmittance was nearly recovered under open-circuit condition, illustrating that high transparency was obtained even in the state of EC gels. With this consideration, devices with low-voltage driven and high optical contrast indicated enormous potential in the area of the electrochromic displays.

3.4. Cycling stability

For practical applications, it is important for ECDs to enhance the stability of EC behavior. To estimate the cycling stability of the prepared ECDs, two-electrode ECDs including $DHV(PF_6)_2$, $HBV(PF_6)_2$ and $poly(HBV(PF_6)_2)$ gels were exposed to the applied square wave voltage between colored and bleached states, because faster coloration than bleaching was achieved in these ECDs (see Fig. 3a–c). The variation of the transmittance in the colored and bleached states for DHV/Fc ECD at 606 nm were given in Fig. 4a. The duration of coloration of ECDs was 30 s at 1.3 V except that of DHV/Fc ECD was 30 s at 1.1 V, and bleaching was tested under open-circuit condition. According to the definition of the △T retention, the DHV/Fc ECD showed an initial ΔT of 47.7%, and 96% of the retention even after 4000 cycles of potential switching, indicating outstanding repetitive operating properties. Similarlly, the initial transmittance change for HBV/Fc ECD was observed as 45.4% at 608 nm, with a 78.9% of the retention after 4000 subsequent cycles, indicating no significant degradation of performance both in colored and bleached state as seen in Fig. 4b. In contrast, the PHBV/Fc ECD showing an initial ΔT of 41.1%, and 70.8% of the retention after 4000 cycles of potential switching, exhibited poorer cyclic stability. The electrochemical performance of viologen-based ECDs utilizing solution, gel or solid electrolyte was summarized in Table 3. Overall, the DHV/Fc ECD based on poly(ionic liquid) gel possessed excellent operational stability under applied bias and a larger ΔT, indicating another effective strategies to improve the cycle stability of simple viologen in ECDs.

4. Conclusions

In this work, we proposed an effective strategy to improve the cyclic stability of viologen with simple molecular structure. Three viologens, including DHV, HBV and PHBV, were successfully synthesized, characterized and incorporated into PIL ion gels containing Fc, giving ITO/ EC gel/ ITO configuration. The DHV, HBV and PHBV-containing ECDs presented good electrochromic properties and revealed a better transmittance change of 47.7%, 45.4% and 41.1% at both detected wavelengths and fast response time within 11.1 s, 10.8 s and 9.2 s, producing a high coloration efficiency of 109.8 cm^2 /C, 106.2 cm^2 /C, 105.7 cm^2 /C, respectively. Especially, the resulting DHV^{2+} exhibited an excellent cyclic stability over 96% of initial transmittance change after 4000 cycles of switching. The results indicated that the introduced PIL can effectively suppress the dimerization of viologen radical cation. It's expected that incorporation of poly(ionic liquid) gel with simple viologen structure could be promising materials for energy-saving smart window or electrochromic displays.

CRediT authorship contribution statement

Xiuxiu Wang: Writing - original draft. **Lijuan Guo:** Visualization. **Shaokui Cao:** Writing - review & editing. **Weizhen Zhao:** Writing - review & editing.

Declaration of Competing Interest

The authors declare that they have no known competing financial interests or personal relationships that could have appeared to influence the work reported in this paper.

Acknowledgements

This work was supported by the National Natural Science Foundation of China (No. 21808224).

Appendix A. Supplementary material

The IR spectrum of VBImBr, poly(VBImBr), $DHV(PF_6)_2$, $HBV(PF_6)_2$ and $poly(HBV(PF_6)_2)$, the ^1H NMR spectrum of poly(VBImBr), $DHV(PF_6)_2$, $HBV(PF_6)_2$ and $poly(HBV(PF_6)_2)$, and the current-time curves of $DHV(PF_6)_2$, $HBV(PF_6)_2$ and $poly(HBV(PF_6)_2)$. Supplementary data to

this article can be found online at https://doi.org/10.1016/j.cplett.2020.137434.

References

[1] M.E. Alberto, B.C. De Simone, S. Cospito, D. Imbardelli, L. Veltri, G. Chidichimo, N. Russo, Chem. Phys. Lett. 552 (2012) 141–145.
[2] Y. Shi, J. Liu, M. Li, J. Zheng, C. Xu, Electrochim. Acta 285 (2018) 415–423.
[3] C. Bechinger, S. Ferrer, A. Zaban, J. Sprague, B.A. Gregg, Nature 383 (1996) 608–610.
[4] J. Jensen, M. Hosel, A.L. Dyer, F.C. Krebs, Adv. Funct. Mater. 25 (2015) 2073–2090.
[5] J. Palenzuela, A. Vinuales, I. Odriozola, G. Cabanero, H.J. Grande, V. Ruiz, ACS Appl. Mater. Interfaces 6 (2014) 14562–14567.
[6] R.T. Wen, G.A. Niklasson, C.G. Granqvist, ACS Appl. Mater. Interfaces 7 (2015) 9319–9322.
[7] G. Cai, A.L.-S. Eh, L. Ji, P.S. Lee, Adv. Sustain. Syst. 1 (2017) 1700074.
[8] S. Bousalem, F.Z. Zeggai, H. Baltach, A. Benyoucef, Chem. Phys. Lett. 741 (2020) 137095.
[9] A.E.X. Gavim, G.H. Santos, E.H. de Souza, P.C. Rodrigues, J.B. Floriano, R.C. Kamikawachi, J.F. de Deus, A.G. Macedo, Chem. Phys. Lett. 689 (2017) 212–218.
[10] B. Gadgil, P. Damlin, T. Ääritalo, C. Kvarnström, Electrochim. Acta 133 (2014) 268–274.
[11] R. Sydam, A. Ghosh, M. Deepa, Org. Electron. 17 (2015) 33–43.
[12] Y. Watanabe, K. Imaizumi, K. Nakamura, N. Kobayashi, Sol. Energy Mater. Sol. Cells 99 (2012) 88–94.
[13] D.M. DeLongchamp, P.T. Hammond, Adv. Funct. Mater. 14 (2004) 224–232.
[14] J. Wang, J.-F. Wang, M. Chen, D.-J. Qian, M. Liu, Electrochim. Acta 251 (2017) 562–572.
[15] G. Wang, X. Fu, J. Deng, X. Huang, Q. Miao, Chem. Phys. Lett. 579 (2013) 105–110.
[16] H.C. Lu, S.Y. Kao, H.F. Yu, T.H. Chang, C.W. Kung, K.C. Ho, ACS Appl. Mater. Interfaces 8 (2016) 30351–30361.
[17] H. Oh, J.K. Lee, Y.M. Kim, T.Y. Yun, U. Jeong, H.C. Moon, ACS Appl. Mater. Interfaces 11 (2019) 45959–45968.
[18] X. Wang, C. Gu, H. Zheng, Y.-M. Zhang, S.X.-A. Zhang, Chem. Asian J. 13 (2018) 1206–1212.
[19] K. Hoshino, R. Nakajima, M. Okuma, Appl. Surf. Sci. 313 (2014) 569–576.
[20] C.M. Correa, S.I.C. de Torresi, T.M. Benedetti, R.M. Torresi, J. Electroanal. Chem. 819 (2018) 365–373.
[21] S.-Y. Kao, C.-W. Kung, H.-W. Chen, C.-W. Hu, K.-C. Ho, Sol. Energy Mater. Sol. Cells 145 (2016) 61–68.
[22] M. Kim, Y.M. Kim, H.C. Moon, RSC Adv. 10 (2020) 394–401.
[23] K.W. Kim, H. Oh, J.H. Bae, H. Kim, H.C. Moon, S.H. Kim, ACS Appl. Mater. Interfaces 9 (2017) 18994–19000.
[24] X. Yang, F. Zhang, L. Zhang, T.F. Zhang, Y. Huang, Y.S. Chen, Adv. Funct. Mater. 23 (2013) 3353–3360.
[25] S. Imaizumi, H. Kokubo, M. Watanabe, Macromolecules 45 (2012) 401–409.
[26] R.X. Dong, S.Y. Shen, H.W. Chen, C.C. Wang, P.T. Shih, C.T. Liu, R. Vittal, J.J. Lin, K.C. Ho, J. Mater. Chem. A 1 (2013) 8471–8478.
[27] S.Y. Kao, H.C. Lu, C.W. Kung, H.W. Chen, T.H. Chang, K.C. Ho, ACS Appl. Mater. Interfaces 8 (2016) 4175–4184.
[28] H. Wang, Z. Wang, J. Yang, C. Xu, Q. Zhang, Z. Peng, Macromol. Rapid Commun. (2018) e1800246.
[29] W. Qian, J. Texter, F. Yan, Chem. Soc. Rev. 46 (2017) 1124–1159.
[30] T.P. Lodge, Science 321 (2008) 50–51.
[31] Y.M. Kim, D.G. Seo, H. Oh, H.C. Moon, J. Mater. Chem. C 7 (2019) 161–169.
[32] D.G. Seo, H.C. Moon, Adv. Funct. Mater. 28 (2018) 1706948.
[33] H. Hwang, S.Y. Park, J.K. Kim, Y.M. Kim, H.C. Moon, ACS Appl. Mater. Interfaces 11 (2019) 4399–4407.
[34] B.S. Lalia, S.S. Sekhon, Chem. Phys. Lett. 425 (2006) 294–300.
[35] B. Singh, S.S. Sekhon, Chem. Phys. Lett. 414 (2005) 34–39.
[36] L.E. Shmukler, Y.A. Fadeeva, E.V. Glushenkova, V.T. Nguyen, L.P. Safonova, Chem. Phys. Lett. 697 (2018) 1–6.
[37] M.D. Green, D. Salas-de la Cruz, Y. Ye, J.M. Layman, Y.A. Elabd, K.I. Winey, T.E. Long, Macromol. Chem. Phys. 212 (2011) 2522–2528.
[38] H. Oh, D.G. Seo, T.Y. Yun, C.Y. Kim, H.C. Moon, ACS Appl. Mater. Interfaces 9 (2017) 7658–7665.
[39] Y. Alesanco, A. Viñuales, G. Cabañero, J. Rodriguez, R. Tena-Zaera, Adv. Opt. Mater. 5 (2017) 1600989.
[40] K. Madasamy, D. Velayutham, V. Suryanarayanan, M. Kathiresan, K.-C. Ho, J. Mater. Chem. C 7 (2019) 4622–4637.
[41] P.M.S. Monk, J. Electroanal. Chem. 432 (1997) 175–179.
[42] Y. Alesanco, A. Viñuales, J. Ugalde, E. Azaceta, G. Cabañero, J. Rodriguez, R. Tena-Zaera, Sol. Energy Mater. Sol. Cells 177 (2018) 110–119.
[43] H.-F. Yu, K.-I. Chen, M.-H. Yeh, K.-C. Ho, Sol. Energy Mater. Sol. Cells 200 (2019) 110020.
[44] K.C. Ho, Y.W. Fang, Y.C. Hsu, L.C. Chen, Solid State Ionics 165 (2003) 279–287.
[45] S.Y. Kao, Y. Kawahara, S. Nakatsuji, K.C. Ho, J. Mater. Chem. C 3 (2015) 3266–3272.
[46] T.M. Benedetti, T. Carvalho, D.C. Iwakura, F. Braga, B.R. Vieira, P. Vidinha, J. Gruber, R.M. Torresi, Sol. Energy Mater. Sol. Cells 132 (2015) 101–106.
[47] G.K. Pande, N. Kim, J.H. Choi, G. Balamurugan, H.C. Moon, J.S. Park, Sol. Energy Mater. Sol. Cells 197 (2019) 25–31.